https://dx.doi.org/10.1016/j.jcsr.2017.11.016

Seismic Design of Beam-Through Steel Frames with Self-Centering Modular Panels

Xinlong Du[1,2], Wei Wang[1,2], Tak-Ming Chan*[,3]

[1]*State Key Laboratory of Disaster Reduction in Civil Engineering, Tongji University, Shanghai 200092, China*

[2]*Department of Structural Engineering, Tongji University, Shanghai 200092, China*

[3]*Department of Civil and Environmental Engineering, The Hong Kong Polytechnic University, Hung Hom, Kowloon, Hong Kong*

ABSTRACT

The beam-through steel frames with self-centering modular panels (BTSF-SCMPs) have been developed as a resilient lateral load resisting system that can address some drawbacks of conventional self-centering systems such as unusual field construction of onsite posttensioning and incompatible deformations relative to gravity framing. This paper outlines a proposed seismic design procedure for this new structural system aimed at achieving specified performance objectives. The design of gravity framing and the lateral load resisting systems are decomposed. Different versions of SCMPs with different recentering stiffness are designed independently to other structural components, and only determined by the dimension and recentering demanding of the structure. During the design of the lateral load resisting system, the designer only need to select the number and version of the SCMPs for each story. A six-story five-bay planar BTSF-SCMPs frame located in a high seismic zone in China was designed using the proposed design approach. Nonlinear pushover analysis and dynamic analysis using ground motions representing two seismic hazard levels were performed for this prototype building to evaluate the design approach.

KEYWORDS Self-centering; Modular panel; Seismic design; Nonlinear analysis

1 Introduction

Conventional structures are designed to dissipate seismic energy through inelastic behavior of structural members, which require expensive repairs, significant business downtime and in some cases building demolition [1]. Thus, the self-centering seismic lateral force resisting systems have been developed to prevent structural damage to non-replaceable structural elements by softening the structural response elastically through gap opening mechanisms [2, 3, 4], adding replaceable energy dissipating elements [5, 6] and through adopting smart materials in connections [7, 8, 9, 10]. The posttensioned (PT) beam-to-column connections adopted in these new systems exhibit nonlinear elastic behavior and can return the structure to its pre-earthquake position. The energy dissipating elements include yielding angles, steel bars, friction devices and steel plate shear walls [3, 4, 11, 12]. Performance-based seismic design approaches have been proposed by different researchers for different kinds of self-centering structures with different performance objectives and their design approaches were verified by nonlinear pushover and time-history analysis [13, 14, 15].

However, examples of self-centering systems used in practice are limited due to complex field construction practices, high initial cost premiums and deformation incompatibility between the self-centering system and gravity framing of the structure [16]. A shop-fabricated self-centering beam moment frame has been developed to simplify the field construction method and eliminate the deformation incompatibility, and computational simulations and experiments have been conducted to examine the performance of this new system [16, 17, 18]. The self-centering modular panel (SCMP) is another self-centering system that can address these problems [19]. The SCMP is a posttensioned steel moment-resisting frame which can be shop fabricated and then be inserted to the bay of the main frame. Several

beam-through steel frames with three types of SCMPs (SCMP1, SCMP2 and SCMP3) have been tested to verify the function of the SCMPs. Wang et al. concluded that SCMP3 has simpler configuration and can reduce the moment demands of the through beams compared with other two types of SCMPs [19]. The SCMPs investigated in this paper all have the same configuration with SCMP3 which only consists of panel beams, panel columns and PT strands. Figs. 1(a and b) show the elevation view of the beam-through steel frame with self-centering modular panels (BTSF-SCMPs) and a test setup of the system. In the figure, the SCMPs are shown with solid lines, and the beam-through steel frame is shown with dotted lines. Details of the SCMP-to-through beam connection can be seen in Fig. 2. Filler plates can be added between the panel beams and the through beams to prevent the pounding between them; and a sloped cutout (shown in Fig. 2(a) but not adopted in Fig. 2(b)) can also be made at the ends of the panel columns to achieve this goal. Note that the stiffeners and bolts are not shown in Fig. 2(a) for clarity and other details can be found in Wang et al. [19]. Since the panel columns have no interaction with the through beams and floor slabs during loading, the SCMP's PT frame expansion during lateral deformation does not affect the floors of the main frame.

1.1 *Beam-Through Steel Frames Behavior*

Wang et al. introduced the tension-only concentrically braced beam-through steel frames and proposed a seismic design procedure aimed at achieving uniform inter-story drift [20, 21]. This system has continuous steel beams and discontinuous steel columns. Wang et al. used semi-rigid through beam-to-column connections. As for the beam-through steel frames in this paper, simple connections are adopted for the through beam-to-column connections to prevent damage of the connections under large deformation. So the details of the through beam-to-columns connections should be different from which

introduced by Wang et al. Tension-only bracings made of very slender flat steel strips serve as the energy dissipating elements. The idealistic response of the beam-through steel frame with tension-only bracings is shown in Fig. 3(a). The notable deteriorating pinched hysteretic behavior is primarily because of bracings' cyclic compression buckling and tension yielding. The plastic deformation of the bracings results in a sharp decrease of the lateral stiffness when the frame returns to nearly zero drift.

1.2 *Self-Centering Modular Panels Behavior*

Wei el al. present the response of SCMPs (Fig. 3(b)) and the methods to calculate the initial stiffness $k_{i,PTF}$ and recentering stiffness k_r [19]. In the following design method of SCMPs, the axial stiffness of panel beams (shown in Fig. 1) will be restricted to be very large compared with the axial stiffness of PT strands (shown in Fig. 1). Also considering that the panel beams will be connected to the through beams near both panel beam ends, so the panel beams will be stiffened by the through beams and the floor slabs. Accordingly, here the axial deformation of the panel beams will be neglected. The following equations are developed based on the equations provided by Garlock [22]. Fig. 4 shows the deformed shape of the PT connections and strands. Decompression means the gap opening phenomenon between the panel beam and panel column. The strands elongation during the gap opening causes an increase in the PT force. If the strands are placed symmetrically about the centroid of the panel beam and the rotation of the two panel columns are the same, then all PT strands experience the same elongation Δ_{PT}. Δ_{PT} can be estimated as:

$$\Delta_{PT} = H_{PB}\theta_r \tag{1}$$

where θ_r = relative rotation between the panel beam and panel column; H_{PB} = depth of the panel beam at the connection. The PT force T_{PT} and the PT connection moment M after decompression can be calculated as follows:

$$T_{PT} = T_0 + k_{PT}\Delta_{PT} = T_0 + k_{PT}H_{PB}\theta_r \tag{2}$$

$$M = \frac{H_{PB}}{2}T_{PT} = \frac{H_{PB}}{2}T_0 + \frac{H_{PB}^2}{2}k_{PT}\theta_r \tag{3}$$

where k_{PT} = axial stiffness of all PT strands per panel beam; T_0 = initial PT force per panel beam. The recentering stiffness k_r can be obtained by using the equations provided by Wei et al. [19] and neglecting the axial shorten of the panel beams. Thus, the recentering stiffness k_r can be approximated as:

$$k_r = \frac{2H_{PB}^2}{H^2}k_{PT} = \frac{2H_{PB}^2}{H^2}\frac{E_{PT}A_{PT}}{L_{PT}} \tag{4}$$

where E_{PT}, L_{PT} and A_{PT} = elastic modulus, length of the PT strands, and total cross-sectional area of PT strands per panel beam, respectively; H = overall height of the SCMP. Equation (4) is valid when the flexural deformation of the panel beams and panel columns can be neglected after decompression. Note that Fig. 3(b) only presents the response of the SCMP when all of its components remain elastic.

1.3 *Combined System Behavior*

The response of the combined BTSF-SCMPs system is shown in Fig. 3(c). Before bracings yielding, the initial stiffness of the system is k_i, which combines the contribution of the SCMP ($k_{i,PTF}$) and bracings (k_b). The SCMP provides the system with relatively large initial stiffness $k_{i,PTF}$ after the bracings experienced large plastic deformation. And the system also maintains the recentering stiffness k_r under relative large drift when the bracings are tensioned to yielding. The SCMP can also recentering the system to its original position with no residual drift after the lateral loads are removed. In this new system, the vertical load is carried by the beam-through steel frames and the lateral load is carried by SCMPs and bracings.

2 **Performance-Based Seismic Design Approach**

As shown above, the beam-through steel frame only carries the vertical load, so it can be designed only considering the gravity load. The major function of the SCMPs is to overcome the P-Δ effects and at the same time they can provide some lateral resistance. So the functions of beam-through steel frame and SCMPs are not correlated. In order to simplify the design procedure, the SCMPs can be designed independently to the beam-through steel frames. The SCMPs can be designed as several versions of shop-fabricated products which have different recentering stiffness. After the design of the beam-through steel frames, the engineers only need to choose the version and number of SCMPs for each story to satisfy the requirements. Then the area of the bracings of each story can be determined by the difference value between the lateral resistance demanding and the lateral resistance contribution of the SCMPs.

As the mechanism of the BTSF-SCMPs system is clarified in the previous section, a design approach in which the target damage state for each structural component, for a given seismic hazard level, can be specified. According to the *Code for seismic design of buildings of China* (GB 50011-2010) [23], the BTSF-SCMPs system is designed for structural performance objectives under two seismic hazard levels, specifically under earthquakes with a 63% and 2~3% probability of exceedance in 50 years (referred to as frequent earthquake and rare earthquake, respectively).

2.1 *Performance Objectives*

The proposed design strategy has 4 main performance objectives (POs), which are defined as follows and are illustrated in Fig. 5. In Fig. 5, V_{wind}, V_{FE}, V_{RE} and V_{MAX} refer to the story shear under wind loads, frequent earthquakes, rare earthquakes and extreme loading conditions, respectively; while Δ_{wind}, Δ_{FE}, Δ_{RE} and Δ_{MAX} indicate the interstory drift under wind loads, frequent earthquakes, rare earthquakes and

extreme loading conditions, respectively. PO 4 should be satisfied during the design of SCMPs and PO 1 to PO 3 should be satisfied in the design of the BTSF-SCMPs system.

1. PO 1: No PT connection decompression under wind loading.

2. PO 2: The BTSF-SCMPs system recenters, and no repair of the system is required after a frequent earthquake. This objective requires all structural components remain elastic under the action of a frequent earthquake. PT connections may or may not decompress under this circumstance. The GB 50011-2010 suggested that peak story drifts should not exceed 0.4% under this hazard level. Recentering is assessed using a residual drift limit of 0.2%, as suggested by Clayton et al. [11].

3. PO 3: System recenters, and only bracings repair is required for the rare earthquakes. Significant yielding only occurs in the bracings; however, all other components of the beam-through steel frames and SCMPs should remain elastic. It is very convenient to replace the bracings after the building recenters to its original configuration. A target story drift limit for this PO is set to 2% to prevent collapse according to the GB 50011-2010.

4. PO 4: In the extreme loading conditions where the system is loaded beyond the target design drift limit of 2%, the panel columns should develop significant inelastic deformations and excessive elongations of the PT strands should be prevented. The formation of plastic hinges at critical panel column sections can be considered as a mechanism that leads to a ductile ultimate behavior of the SCMPs. This PO is adopted to prevent sudden loss of the strength and stiffness of the system, when the system is loaded beyond its maximum design drift [14]. Residual drifts may occur and the entire SCMPs which have experienced inelastic deformations could be replaced after a disaster to repair the system.

2.2 *Design of SCMPs*

The most important design parameter of a SCMP is its recentering stiffness k_r (Equation (4) and in Fig. 3(b)). Firstly, a series of k_r should be selected according to the requirements of the building's recentering and engineering judgment. Then the SCMPs can be designed to achieve the different target values of k_r, while satisfying the requirements of the PO 3 and PO 4.

The height and length of the SCMPs can be determined based on the beam-through steel frames' story height and bay length. Therefore, the H and L_{PT} in Equation (4) are known. Then the recentering stiffness of a SCMP is only controlled by panel beam depth H_{PB} and PT strands' total cross-sectional area A_{PT}. Here, the initial PT force T_0 is suggested to be 30% ~ 50% of its ultimate strength, which can provide a relative large initial PT force, while the PT strands can experience a relative large deformation. After H_{PB}, A_{PT} and T_0 are selected, the panel beams and panel columns can be designed to satisfy the following five controlling conditions:

1. The parameter $\alpha = k_{PB}/(k_{PB}+k_{PT})$ should be no smaller than 0.9. Here k_{PB} is the axial stiffness of the panel beam. This controlling condition can make sure the axial stiffness of the panel beam is much larger than the axial stiffness of the PT strands. Moreover, given the panel beams are stiffened by the through beams and the floor slabs, the axial compression deformation of the panel beams can be neglected when developing the Equations (1) to (4).

2. The parameter $\beta = k_{i,PTF}/(k_{i,PTF}+k_r)$ should be no smaller than 0.9. This can make sure the flexural stiffness of the SCMP is much larger than k_r, so that the deformation of the SCMP after decompression is mainly due to the rotation of the PT connections instead of the flexural deformation of the panel beams and panel columns. This parameter can be used to amend the k_r obtained from Equation (4) when the panel

beams and panel columns cannot be treated as rigid bodies after decompression. Note that shear deformation in the panel zones of the PT connections was neglected, which can be achieved by adequate reinforcement on these areas.

3. All components of the SCMPs remain elastic until the story drift is 2%. This is established to satisfy the PO 3. Considering the geometry relationship between SCMPs and beam-through steel frames, when the story drift is 2%, the corresponding PT connection relative rotation will be larger than 2%. Here θ_{r1} is defined as the value of the PT connection rotation when the story drift is 2%, and can be calculated after the panel beam depth H_{PB} is selected. By substitute θ_{r1} to Equation (3), the PT connection moment when the story drift equals to 2% can be obtained and be denoted as M_1. Here M_1 is required to be smaller than the first yield moment capacity of the panel columns and panel beams.

4. The panel columns reaches whole section yielding and plastic hinges appear before the PT strands reach the first yield point. This is established to satisfy PO 4 which makes sure the yielding and fracture will not occur to the PT strands even if the system is over loaded. Here θ_{r2} is defined as the value of the PT connection rotation when the PT strands reach the first yield point, and can be obtained by using Equation (2). By substitute θ_{r2} to Equation (3), the PT connection moment when the PT strands reach the first yield point can be obtained and be denoted as M_2. Here M_2 is required to be larger than the whole section yield moment capacity of the panel columns.

5. The panel beam section should reasonably fit the corresponding number of PT strands within its depth.

When the selected sections of panel beams and panel columns satisfy the above five controlling conditions, the design of a SCMP is complete. However, if the controlling conditions cannot be satisfied all the time, the H_{PB}, A_{PT} and T_0 can be re-selected.

2.3 *Design Procedure of BTSF-SCMPs*

A proposed design procedure for the BTSF-SCMPs system is outlined as follows and illustrated in Fig. 6.

1. Step1: Given the basic design information provided, the layout and sections of columns and through beams can be designed for gravity loads. The limit value of axial compression ratio of structural columns under gravity loads is set below 0.3 to ensure the columns would not yield when subjected to the vertical component of concentric brace forces under rare earthquakes [21, 24].

2. Step 2: Select the version and number of SCMPs for each story. To ensure recentering following the frequent or rare earthquakes, each story should have a positive recentering lateral stiffness, K_r, considering the negative stiffness due to P-Δ effects [15]. Accordingly, the following Equation (5) should be checked story by story to make sure that the sum of the recentering stiffness of all SCMPs per story can overcame the stiffness loss caused by P-Δ effects.

$$K_r = \sum \beta k_r - \frac{P}{h} \geq 0 \tag{5}$$

where $\Sigma\beta k_r$ = sum of the recentering stiffness of all SCMPs at a particular story; h = story height; P = portion of the P-Δ load that must be resisted by the SCMP at a particular story. Here, β is used to consider the reduction of the recentering stiffness due to the flexural deformation of the panel beams and panel columns after decompression.

3. Step 3: Determine the seismic base shear under frequent earthquakes for use in the design of bracings.

The GB 50011-2010 gives the following equation to calculate the base shear:

$$V = 1.3 \times \alpha_1 G_{eq} \tag{6}$$

where the coefficient 1.3 refers to the partial safety factor of the horizontal earthquake action; G_{eq} denotes the effective seismic weight; α_1 means the seismic influence coefficient under frequent earthquakes, which is determined by the seismic intensity, damping ratio, characteristic site period T_g and the fundamental period of the structure T_1. According to the *Load code for the design of building structures of China* (GB 50009-2012) [25], T_1 can be conservatively estimated as:

$$T_1 = 0.1n \tag{7}$$

where n is the number of floors.

4. Step 4: Determine the seismic load distribution for use in the design of bracings. The GB 50011-2010 suggests the equivalent lateral force distribution for buildings under the condition that the building is not taller than 40 m, that the shear deformation dominates and that the mass and stiffness distribution is relatively uniform.

5. Step 5: Design the bracings using the lateral load distribution and base shear calculated in Steps 3 and 4. The bracings is designed to remain elastic under this loading condition. The lateral load resistance of the SCMPs is considered during the design and conservatively the lateral forces of decompression V_{dec} are selected to be their contributions for simplicity of calculations. The drift limit of PO 2 should be satisfied in this step.

6. Step 6: Check that design meets the PO 1. Here, the stiffness of the SCMP is considered to be its initial stiffness $k_{i,PTF}$. The lateral load that the SCMP resists should be smaller than its lateral force of decompression.

7. Step 7: Check that design meets the drift limit of PO 3 using nonlinear time-history analysis.

3 **Design example of a six-story planar frame**

In order to illustrate how the proposed design procedure is carried out, a six-story five-bay planar BTSF-SCMPs was considered as a prototype building. The building was assumed to be located in Urumqi and was designed on the basis of relevant design provisions of China. The prototype building had uniform story heights of 3.34 m and bay lengths of 3 m. All the through beam-to-column connections and column based are hinged. Equivalent line gravity loads were set to be 36 kN/m for the through beams of 1st to 5th floors, while 30 kN/m for the through beams of 6th floor, respectively. These equivalent loads considered the dead loads and live loads. Note that the wind loads were not considered in the design because this is a planar frame with no walls for the wind loads' action, so the performance objective PO 1 was not checked.

3.1 *Design results of SCMPs*

The height and length of the SCMPs were selected to be about 3 m and 2.6 m based on the dimensions of the main frame. The panel beams and panel columns were designed using the Q235 steel (the nominal yielding point is 235 MPa). The PT strands were 15.2-mm-diameter seven-wire strands with an ultimate tensile strength of 1,860 MPa. Here the yielding point of the PT strands was established as 90% of its ultimate strength. The depth of the panel beams was set to be 300 mm, and different recentering stiffness k_r could be achieved by changing the number of PT strands per panel beam. Table 1 provides the design details and properties of four well-designed SCMPs, including the number of PT strands per panel beam N_{PT}, the cross-sectional area of PT strands per panel beam A_{PT}, the ratio of initial PT force to ultimate strength of the PT strands T_0/T_u, the lateral force of decompression V_{dec}, the first yield moment capacity of the panel column M_e, the whole section yield moment capacity of the panel column M_p, the PT

connection moment M_1 corresponding to θ_{r1}, the PT connection moment M_2 corresponding to θ_{r2} and so on. Here θ_{r1} was 2.5% and θ_{r2} was 4.8%, which were obtained by using the methods provided in Section 2.2. All panel beams' length was 2 m and all panel columns' length was 3 m. It can be verified that the design results meet all the five design controlling conditions of SCMPs. From Wang el al.'s experimental experience, the panel beam depth of 300 mm is enough to fit up to 8 PT strands [19].

3.2 *Design results of BTSF-SCMPs*

The through beams, columns and bracings were designed using the Q345 steel (the nominal yielding point is 345 MPa). The through beams adopted the welded H-sections and the columns adopted the cold-formed square-tubes. Their sections were selected based on gravity loads only and the design results are shown in Table 2.

When choosing the version and number of SCMPs for each story, the sum of the recentering stiffness of the SCMPs per story should be larger than the negative stiffness caused by the P-Δ effect. In order to transmit the lateral force effectively, the SCMPs are required to place continuously story by story, that is if one specific bay of a story has a SCMP, the corresponding bay of the adjacent lower story should have a SCMP. The selection results and layout of the SCMPs are shown in Table 3.

The maximum seismic influence coefficient under frequent earthquakes α_{max}, the damping ratio, the characteristic site period T_g and the estimated fundamental period of the structure T_1 were selected to be 0.16, 0.04, 0.4 s and 0.6 s, respectively, according to the GB 50011-2010 and GB 50009-2012. Therefore, the seismic influence coefficient under frequent earthquakes α_1 were obtained as 0.1179 according to GB 50011-2010. Note that the parameter α_{max} for this site represents some of the largest seismic hazard in China. The story shears were determined after the base shear and seismic load distribution were obtained

based on the GB 50011-2010. The design results and layout of the bracings are shown in Table 4 and Fig. 7, respectively. Here V_e means the elastic strength of the tensile bracings of a particular story, and A_b means the cross-sectional area of the tensile bracings.

4 Verification of design approach

4.1 *Analytical Model Development*

The BTSF-SCMPs designs were modeled using the software ABAQUS. The through beams, panel beams and panel columns were modeled using beam elements (B21). The columns were modeled using truss elements (T2D2). The bracings and strands were modeled using a series of tension-only truss elements (T2D2 with no-compression material property). The PT connection model developed by Clayton et al. was adopted to simulate the gap opening mechanisms [15, 26]. The prestress of PT strands were applied by reducing the temperature of the corresponding truss elements after giving them an expansion coefficient. The panel beams and panel columns were modeled using an essentially elasto-perfectly plastic model. Other components were modeled using a bilinear inelastic model with a strain hardening modulus that is 1% of the initial young's modulus.

All the mass of the structural components and the equivalent line gravity loads were considered as the seismic weight. The equivalent line gravity loads on the through beams were applied by amplifying the density of the through beams so that the equivalent weight of the through beams equal to the real weight of themselves plus the equivalent line gravity loads. Theses gravity loads would contribute to P-Δ effects on the structure.

4.2 *Pushover Analysis Results*

Pushover analysis for the prototype building was performed to capture the monotonic force-deformation relation. The inverted triangular load pattern was applied to the structure. Fig. 8 shows the pushover curve of the prototype building. Along with the increase of the lateral loads, PT connections decompression, bracings yielding, panel columns yielding and panel columns' plastic hinges occurred in sequence. Significant stiffness degradation was observed at a roof drift of about 0.6%, which was caused by the bracings yielding. Significant strength degradation was observed at a roof drift of about 1.78%, which was due to the formation of plastic hinges in the panel columns and the P-Δ effects. Fig. 9 shows the interstory drifts under different roof drifts during the loading. After bracings yielding, the deformation gradually concentrated on the 3rd story, which resulted in yielding of the panels columns in the 3rd story at large deformation. However, the panel columns in the 3rd story remained elastic when the story drift reached 2%, which satisfy the PO 3. In addition, all other components of the beam-through steel frames and SCMPs except for the bracings remain elastic under story drift of 2%. At last, the story drift of the 3rd story reached 9% while the PT strands still remained elastic, which satisfy the PO 4. So when the system is loaded beyond the target design drift limit of 2% in the extreme loading conditions, the panel columns will develop significant plastic hinges, and the PT strands will not yield or fracture. This proved that a ductile ultimate response with no sudden loss of strength and stiffness of SCMPs was achieved.

4.3 *Nonlinear Dynamic Analysis Results*

Two real ground motions (1940 El Centro (N-S) and 1976 Tangshan (E-W)) and one design spectrum compatible artificial ground motion were adopted to run the nonlinear dynamic analysis. Theses ground motions were scaled to peak accelerations of 70 cm/s^2 and 400 cm/s^2 to represent the frequent earthquakes

and rare earthquakes, respectively, according to the GB 50011-2010. Damping was modeled using Rayleigh damping of 4% for frequent earthquakes and 5% for rare earthquakes as suggested by the GB 50011-2010. The analysis were performed for the total duration of each earthquake record with additional zero-acceleration padding to allow for free vibration decay and to capture residual deformation of the structure.

Fig. 10 and Fig. 11 show typical response histories for the prototype building subjected to the Tangshan ground motion under frequent and rare earthquakes, respectively. The first story response under a frequent earthquake was essentially linear elastic, while the first story response under a rare earth quake exhibited the flag-shaped hysteresis with no residual drift, which is typical of the self-centering systems. Fig. 12 and Fig. 13 show the maximum interstory drifts under frequent and rare earthquakes. Considering the geometry relationship and material property of the bracings, it can be concluded that bracings will start yield under story drift of 0.34% according to the equations provided by Wang et al. [21]. Therefore, Fig. 12 can demonstrate that all bracings remained elastic under frequent earthquakes, and that the maximum story drifts of each story under frequent earthquakes did not exceed the drift limit of 0.4%, which met the performance objective PO 2. Only bracings experienced inelastic deformation under rare earthquakes and the maximum story drifts of each story did not exceed the drift limit of 2% (shown in Fig. 13), which met the performance objective PO 3. Fig. 14 shows that the residual story drift of each story following the rare earthquakes was smaller than 0.2%, which proved that the building can recenter after a significant inelastic deformation.

The results of the nonlinear dynamic analysis demonstrated that the BTSF-SCMPs system developed relatively uniform inter-story drifts under frequent and rare earthquakes (Fig. 12 and Fig. 13) and the

maximum drifts satisfied the requirements of the POs. The results of the pushover analysis showed that when the system was overloaded in an extreme condition severer than a rare earthquake, the story drift may concentrate in individual stories. However, in this condition the plastic hinges can occur in the panel columns and dissipate seismic energy as a seismic fortification line, which can provide the system with an ultimate ductile mechanism. These all proved that the proposed design approach of this new structural system is reasonable.

5 Conclusions

The behavior of the BTSF-SCMPs system has been described. The shop-fabricated SCMPs are easy to design, fabricate and install to the beam-through steel frames. The SCMPs expansion caused by gap opening will not interfere the deformation of the floors. This paper outlined a performance-based design approach for the BTSF-SCMPs system. The SCMPs were designed independently to the BTSF-SCMPs system, which can simplify the design procedure significantly. The performance objectives were outlined, design criteria were given, and a step-by-step design procedure was introduced in detail. A six-story five-bay planar BTSF-SCMPs building was designed according to the proposed design procedure. The results of time-history analysis of the prototype building show that the story drift limits and residual drift limits of PO 2 and PO 3 were satisfied. The results of nonlinear pushover analysis show that the well-designed SCMPs can remain elastic up to 2% story drift and that the panel columns can develop plastic hinges before yielding of the PT strands. It is demonstrated that the innovative BTSF-SCMPs system and the proposed design procedure are effective and reliable means to enhance the seismic resilience of buildings.

Acknowledgements

The authors are grateful for the support from the Natural Science Foundation of China (NSFC) with Grant

No. 51778459 and the Chinese National Engineering Research Center for Steel Construction (Hong Kong Branch) at the Hong Kong Polytechnic University. The financial support from the Hong Kong Polytechnic University (PolyU: 1-ZE50/G-YBHV) is also gratefully acknowledged.

References

[1] Chancellor N B, Eatherton M R, Roke D A, et al. Self-centering seismic lateral force resisting systems: high performance structures for the city of tomorrow. Buildings, 2014, 4(3): 520-548.

[2] Ricles J M, Sause R, Peng S W, et al. Experimental evaluation of earthquake resistant posttensioned steel connections. Journal of Structural Engineering, 2002, 128(7): 850-859.

[3] Christopoulos C, Filiatrault A, Uang C M, et al. Posttensioned energy dissipating connections for moment-resisting steel frames. Journal of Structural Engineering, 2002, 128(9): 1111-1120.

[4] Garlock M M, Ricles J M, Sause R. Experimental studies of full-scale posttensioned steel connections. Journal of Structural Engineering, 2005, 131(3): 438-448.

[5] Khador, M. and **Chan, T.-M.** (2016). Cyclic behaviour of external diaphragm joint to CHS column with built-in replaceable links. Steel Construction – Design and Research, 9(4), 331-338, Ernst & Sohn.

[6] Quan, C., Wang, W., **Chan, T.-M.*** and Khador, M. (2017). FE modelling of replaceable I-beam-to-CHS column joints under cyclic loads. Journal of Constructional Steel Research, 138, 221-234.

[7] Wang, W., Chan, T.-M.*, Shao, H.L and Chen, Y.Y. (2015). Cyclic behavior of connections equipped with NiTi shape memory alloy and steel tendons between H-shaped beam to CHS column. Engineering Structures, 88, 37-50, Elsevier.

[8] Wang, W., Chan, T.-M.* and Shao, H.L (2015). Seismic performance of beam-column joints with SMA tendons strengthened by steel angles. Journal of Constructional Steel Research, 109, 61-71, Elsevier.

[9] Wang, W., Chan, T.-M.* and Shao, H.L. (2015). Numerical investigation on I-beam to CHS column connections equipped with NiTi shape memory alloy and steel tendons under cyclic loads. Structures, 4, 114-124, Elsevier.

[10] Cheng Fang, Wei Wang*, Ce He, Yiyi chen. (2017). "Self-centring behaviour of steel and steel-concrete composite connections equipped with NiTi SMA bolts." Engineering Structures, 150: 390-408.

[11] Clayton P M, Winkley T B, Berman J W, et al. Experimental investigation of self-centering steel plate shear walls. Journal of structural engineering, 2011, 138(7): 952-960.

[12] Wolski M, Ricles J M, Sause R. Experimental study of a self-centering beam–column connection with bottom flange friction device. Journal of Structural Engineering, 2009, 135(5): 479-488.

[13] Garlock M M, Sause R, Ricles J M. Behavior and design of posttensioned steel frame systems. Journal of Structural Engineering, 2007, 133(3): 389-399.

[14] Kim H J, Christopoulos C. Seismic design procedure and seismic response of post-tensioned self-centering steel frames. Earthquake Engineering & Structural Dynamics, 2009, 38(3): 355-376.

[15] Clayton P M, Berman J W, Lowes L N. Seismic design and performance of self-centering steel plate shear walls. Journal of structural engineering, 2011, 138(1): 22-30.

[16] Maurya A, Eatherton M R. Self-centering beams with resilient seismic performance. Structures Congress 2014. 2014: 2442-2453.

[17] Darling S C, Eatherton M R, Maurya A. Self-Centering Beams for Seismically Resilient Moment Frames. Structures Congress 2013: Bridging Your Passion with Your Profession. 2013: 1701-1712.

[18] Maurya A, Eatherton M R. Experimental study of the restoring force mechanism in the self-centering beam (SCB). Frontiers of Structural and Civil Engineering, 2016, 10(3): 272-282.

[19] Wang W, Du X, Zhang Y, et al. Experimental Investigation of Beam-Through Steel Frames with Self-Centering Modular Panels. ASCE Journal of Structural Engineering, 2017, 143(5): 04017006.

[20] Wang W, Zhou Q, Chen Y, et al. Experimental and numerical investigation on full-scale tension-only concentrically braced steel beam-through frames. Journal of Constructional Steel Research, 2013, 80: 369-385.

[21] Wang W, Zou C, Chen Y, et al. Seismic design of multistory tension-only concentrically braced beam-through frames aimed at uniform inter-story drift. Journal of Constructional Steel Research, 2016, 122: 326-338.

[22] Garlock M M. 2002. Design, analysis, and experimental behavior of seismic resistant post-tensioned steel moment resisting frames. Ph.D. dissertation, Dept. of Civil and Environmental Engineering, Lehigh Univ., Bethlehem, PA.

[23] Ministry of Housing and Urban–Rural Development of China, Code for Seismic Design of Buildings, GB50011–2010 (Beijing, China) 2010.

[24] Wang W, Zhou Q, Chen Y, et al. Seismic performance of floor-by-floor assembled steel braced structures with stiffened connections. The IES Journal Part A: Civil & Structural Engineering, 2013, 6(2): 112-118.

[25] Ministry of Housing and Urban–Rural Development of China, Load Code for Design of Building Structures, GB50009–2012 (Beijing, China) 2012.

[26] Clayton P M, Berman J W, Lowes L N. Subassembly testing and modeling of self-centering steel plate shear walls. Engineering Structures, 2013, 56: 1848-1857.

List of Figure Captions

Fig. 1 (a) Typical BTSF-SCMPs elevation; (b) Test setup of a BTSF-SCMP system

Fig. 2 Details of the SCMP-to-through beam connection

Fig. 3 System force-displacement idealized responses

Fig. 4 Deformed shape of PT connections and strands

Fig. 5 Performance-based design objectives for BTSF-SCMPs

List of Table Captions

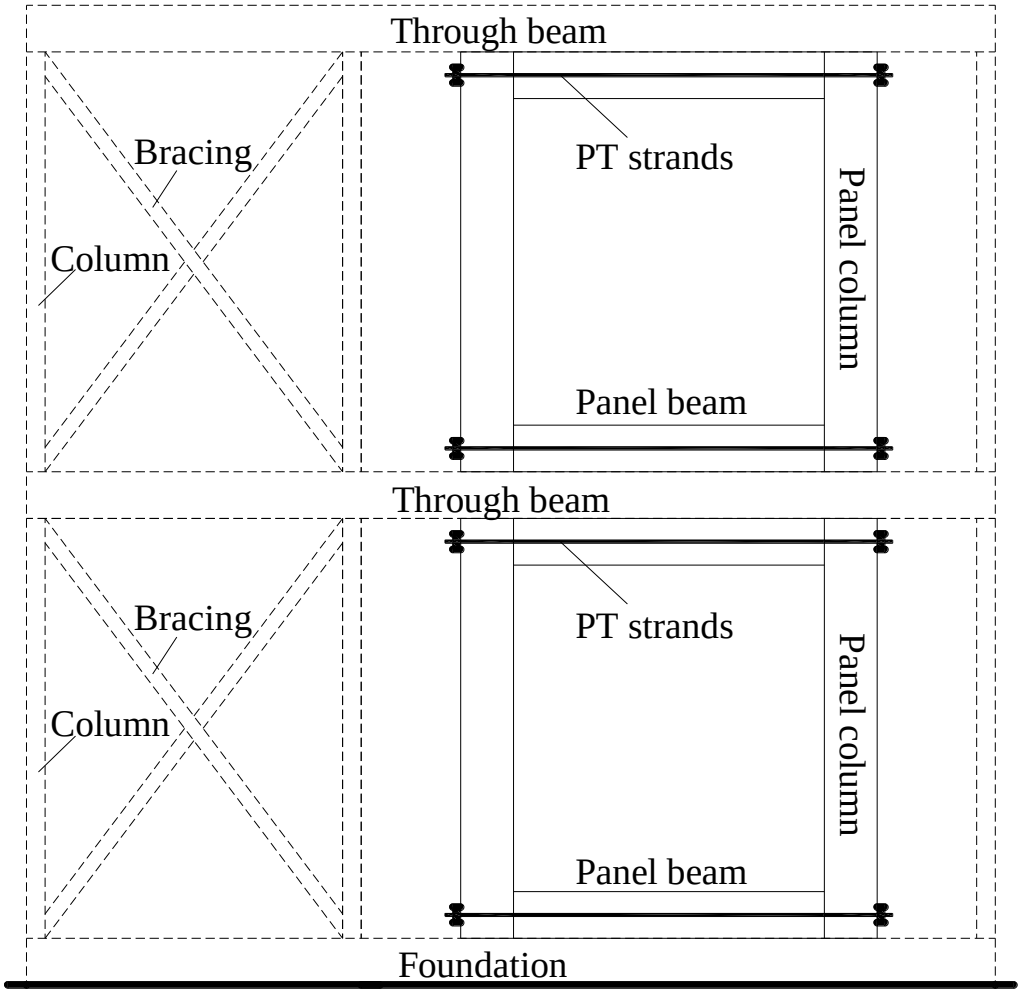

(a)

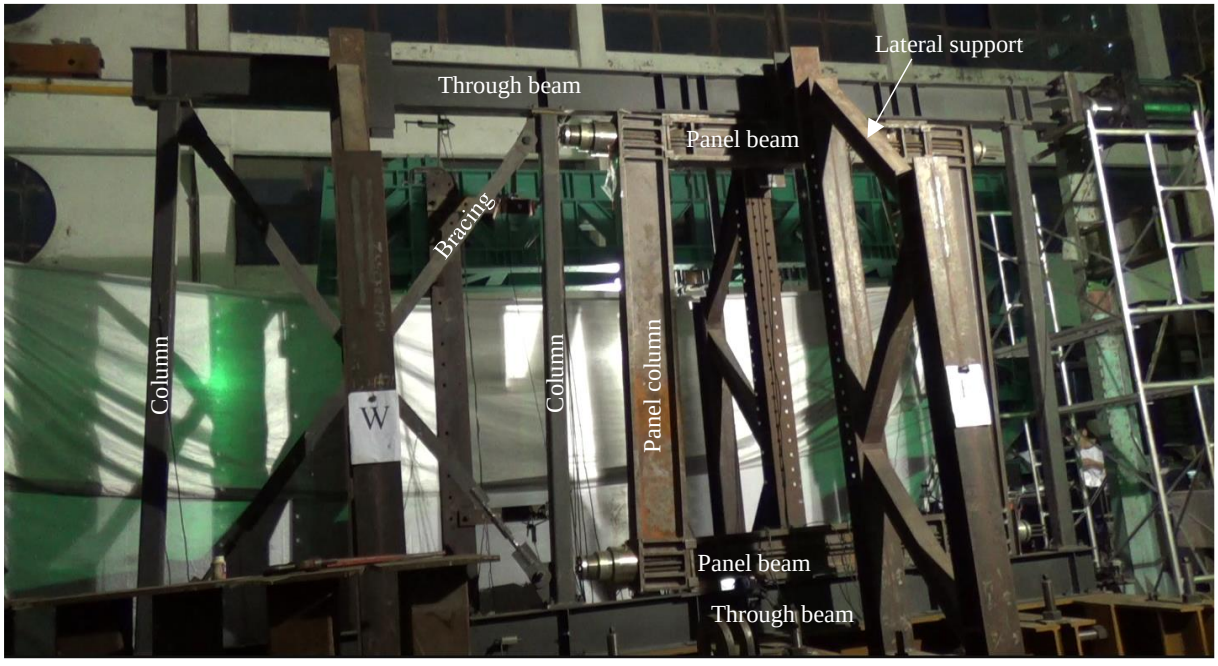

(b)

Fig. 1 (a) Typical BTSF-SCMPs elevation; (b) Test setup of a BTSF-SCMP system

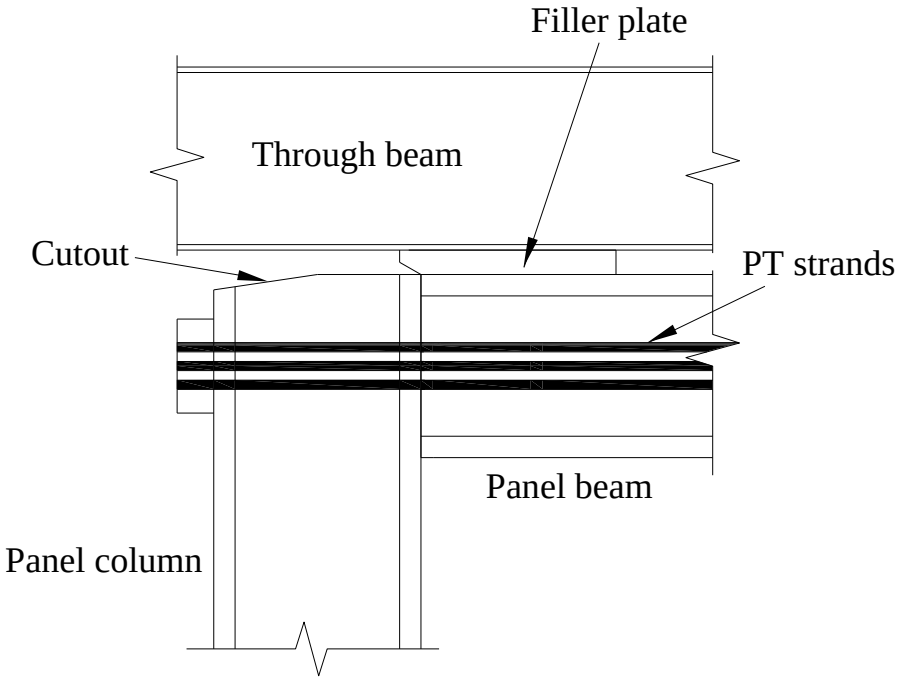

(a)

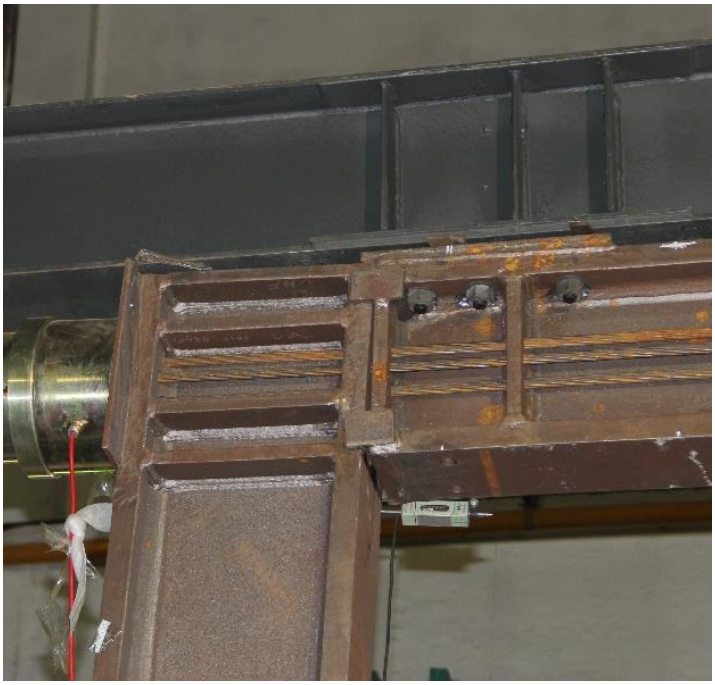

(b)

Fig.2 Details of the SCMP-to-through beam connection

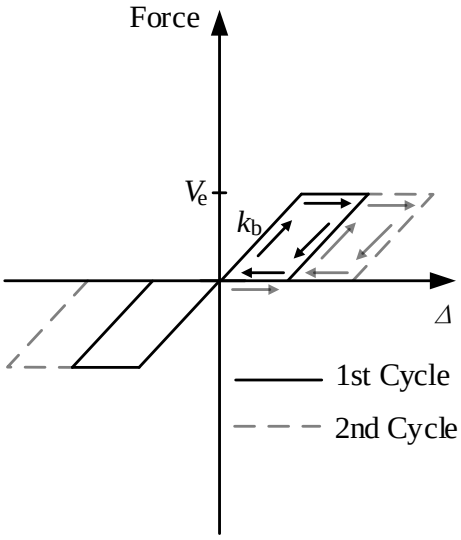

(a) BTSF response

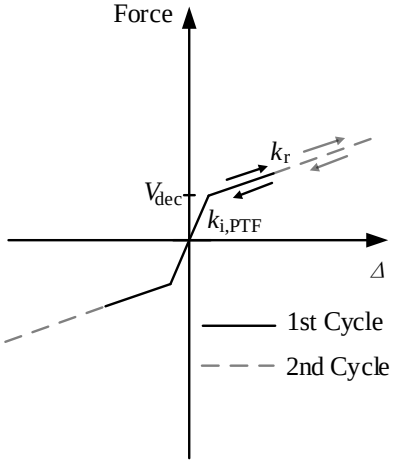

(b) SCMP response

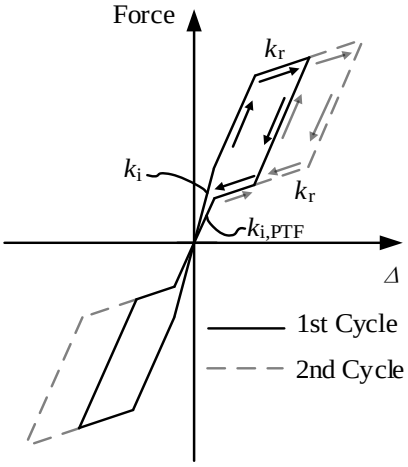

(c) BTSF-SCMP response

Fig.3 System force-displacement idealized responses

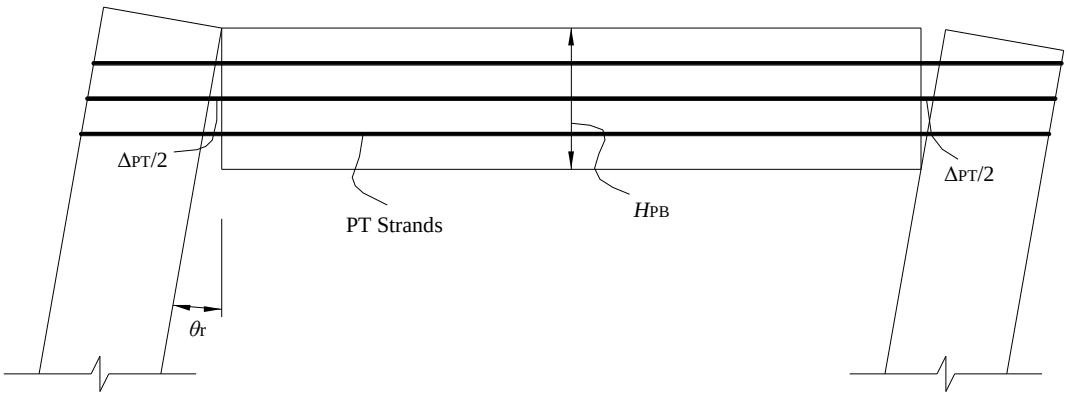

Fig.4 Deformed shape of PT connections and strands

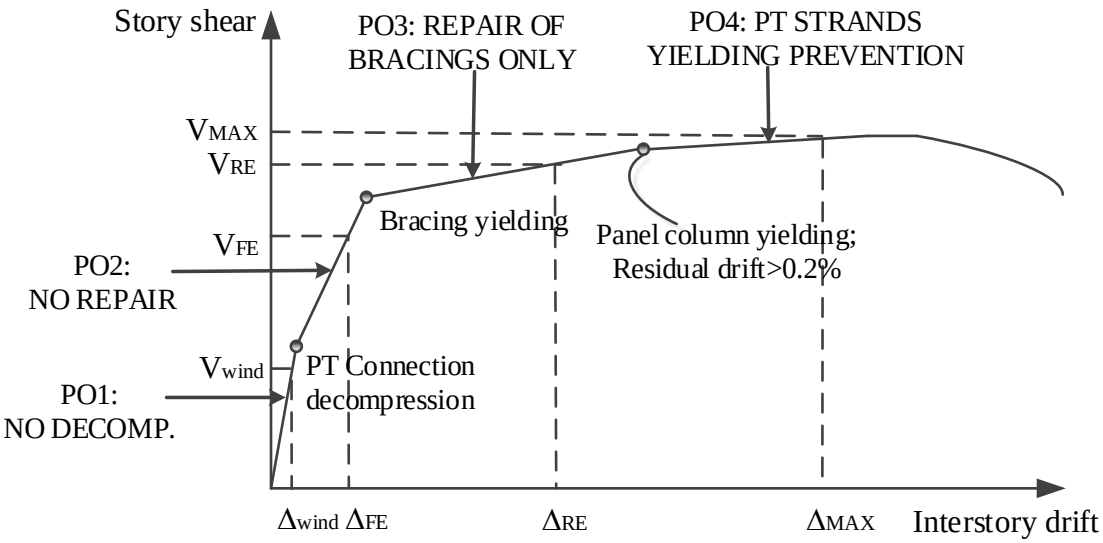

Fig. 5 Performance-based design objectives for BTSF-SCMPs

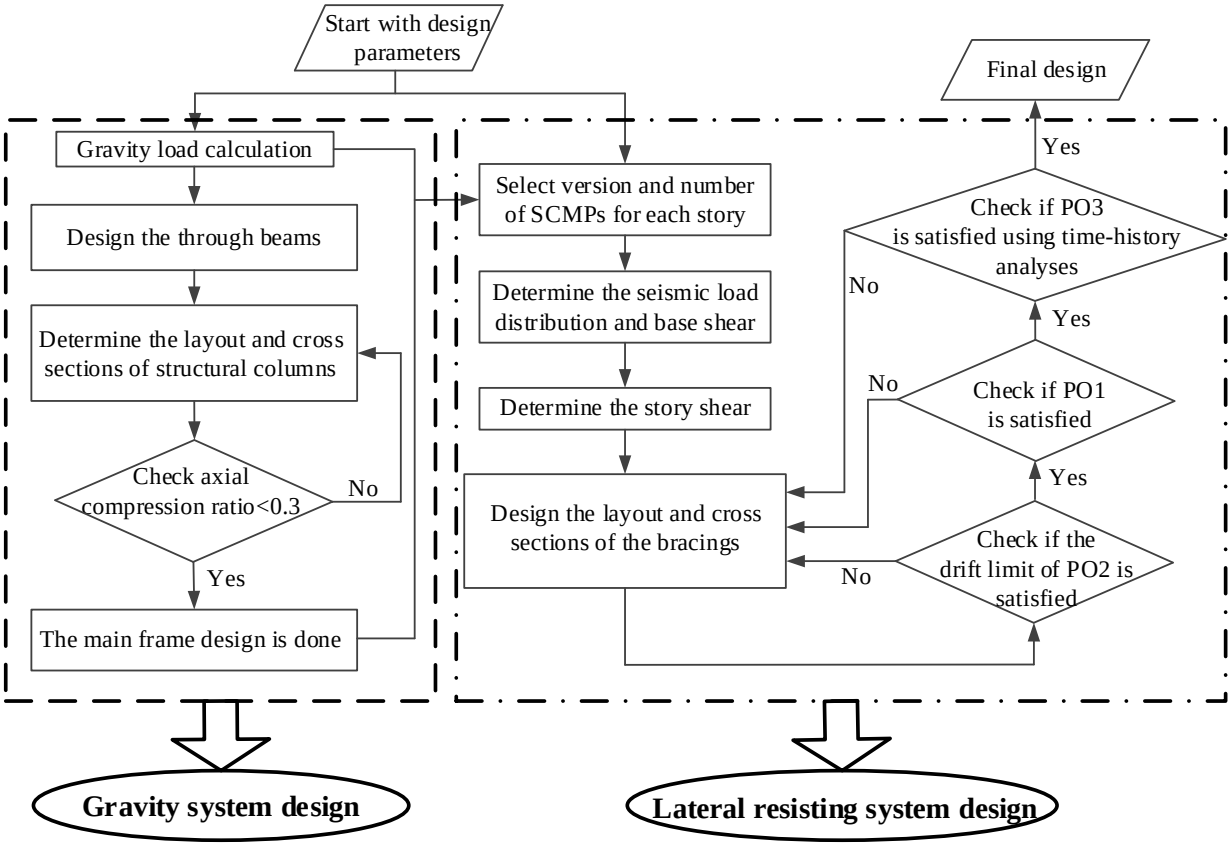

Fig. 6 Flow chart of the proposed design procedure

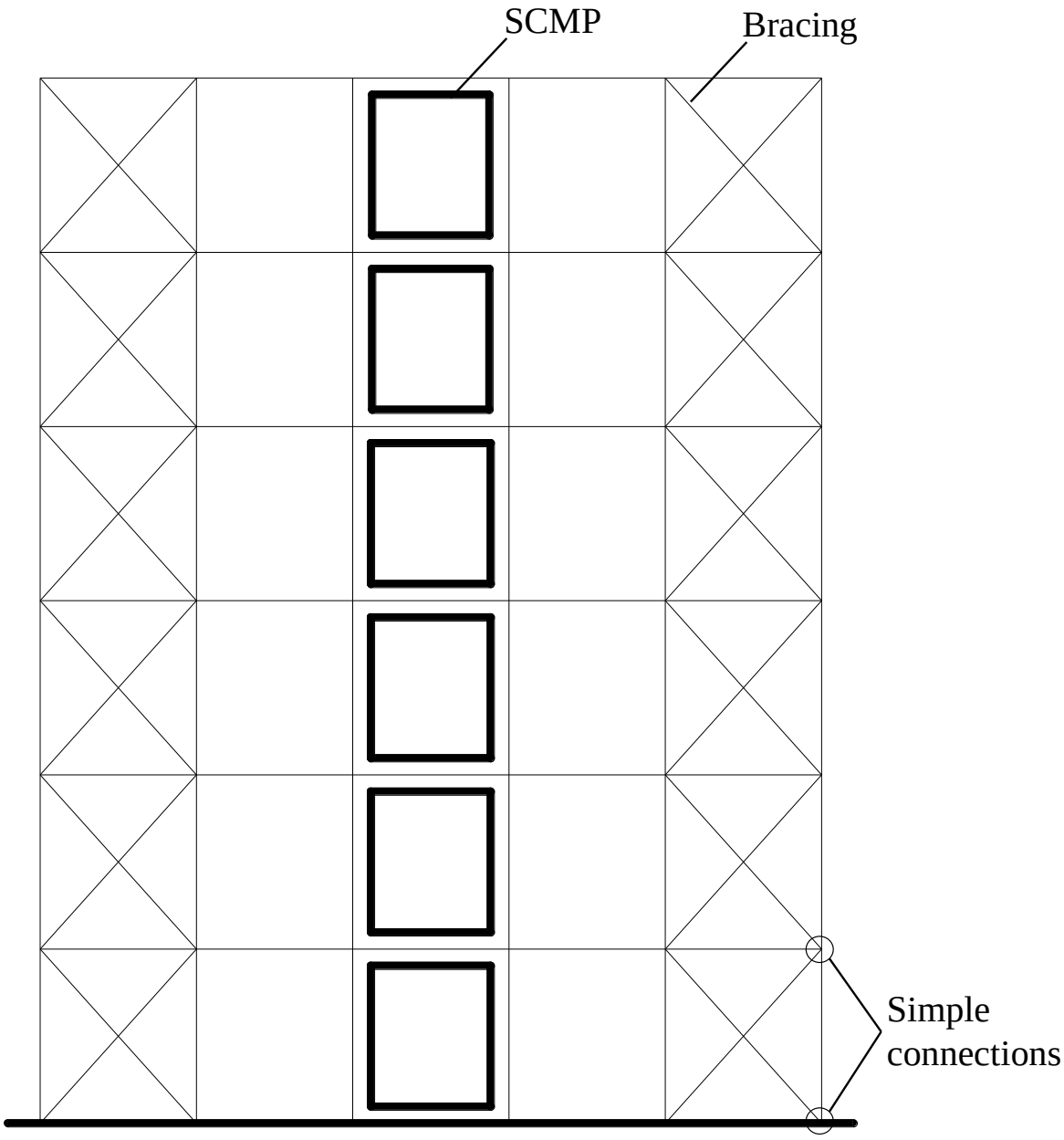

Fig. 7 Design layout of the bracings and SCMPs

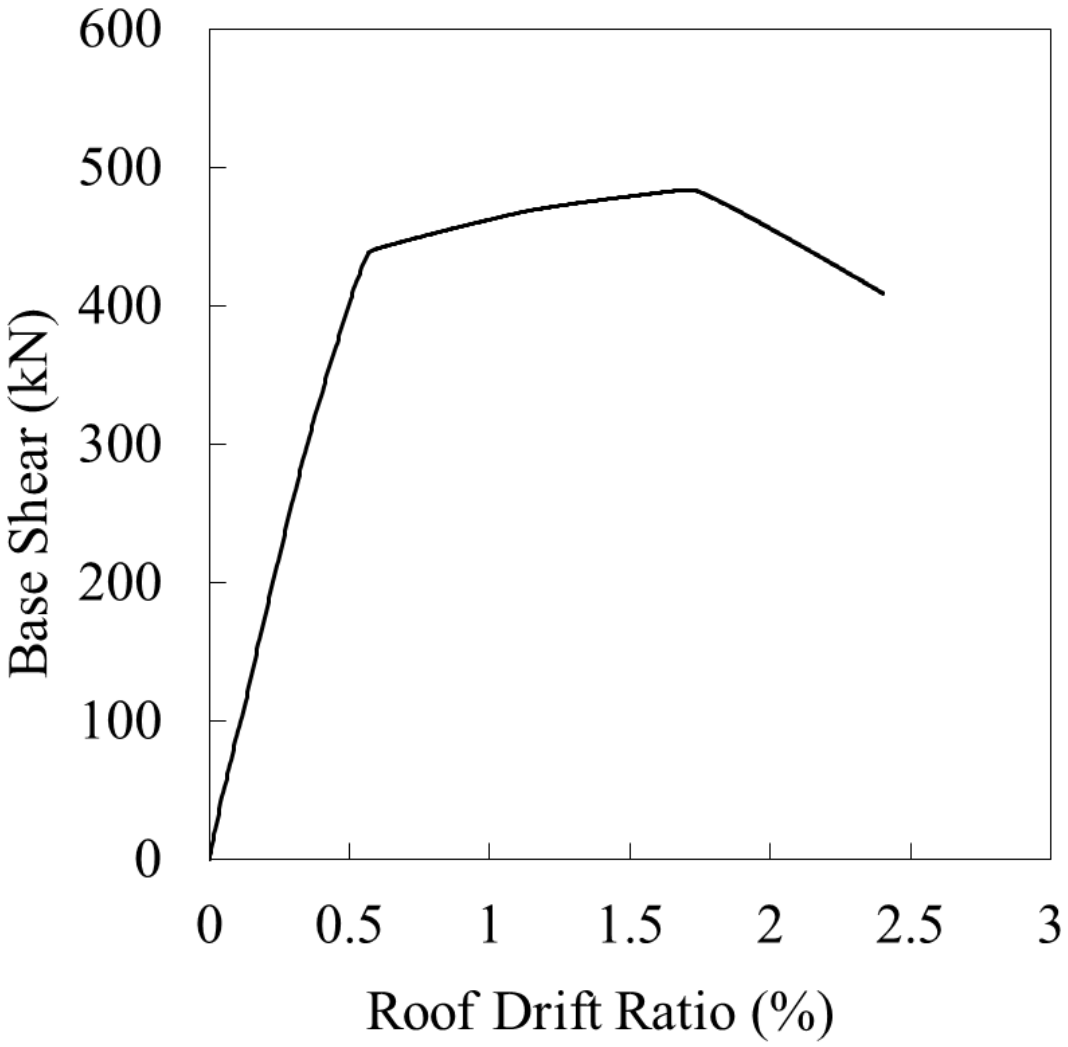

Fig. 8 Pushover curve of the prototype building

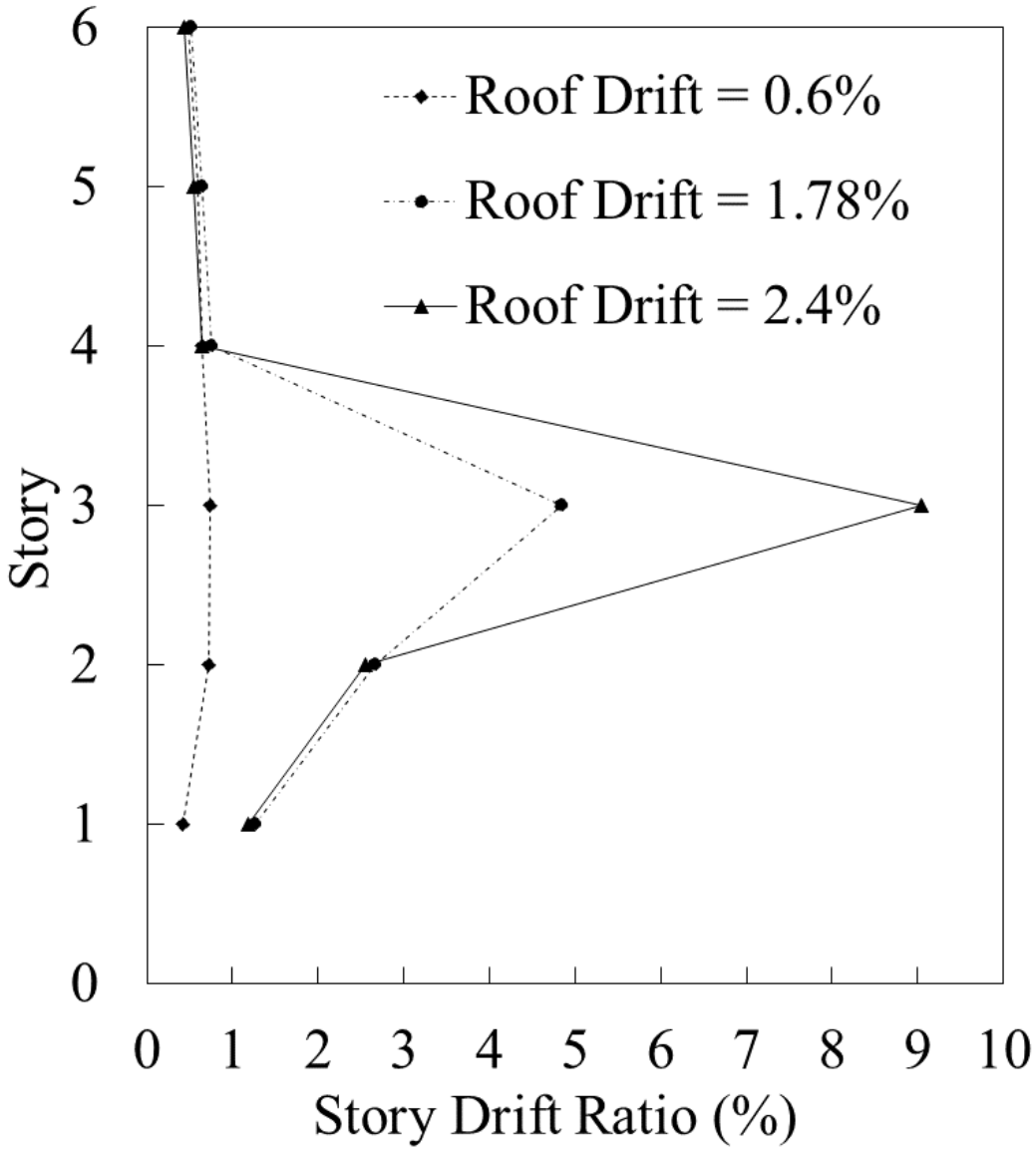

Fig. 9 Story drifts under different roof drifts

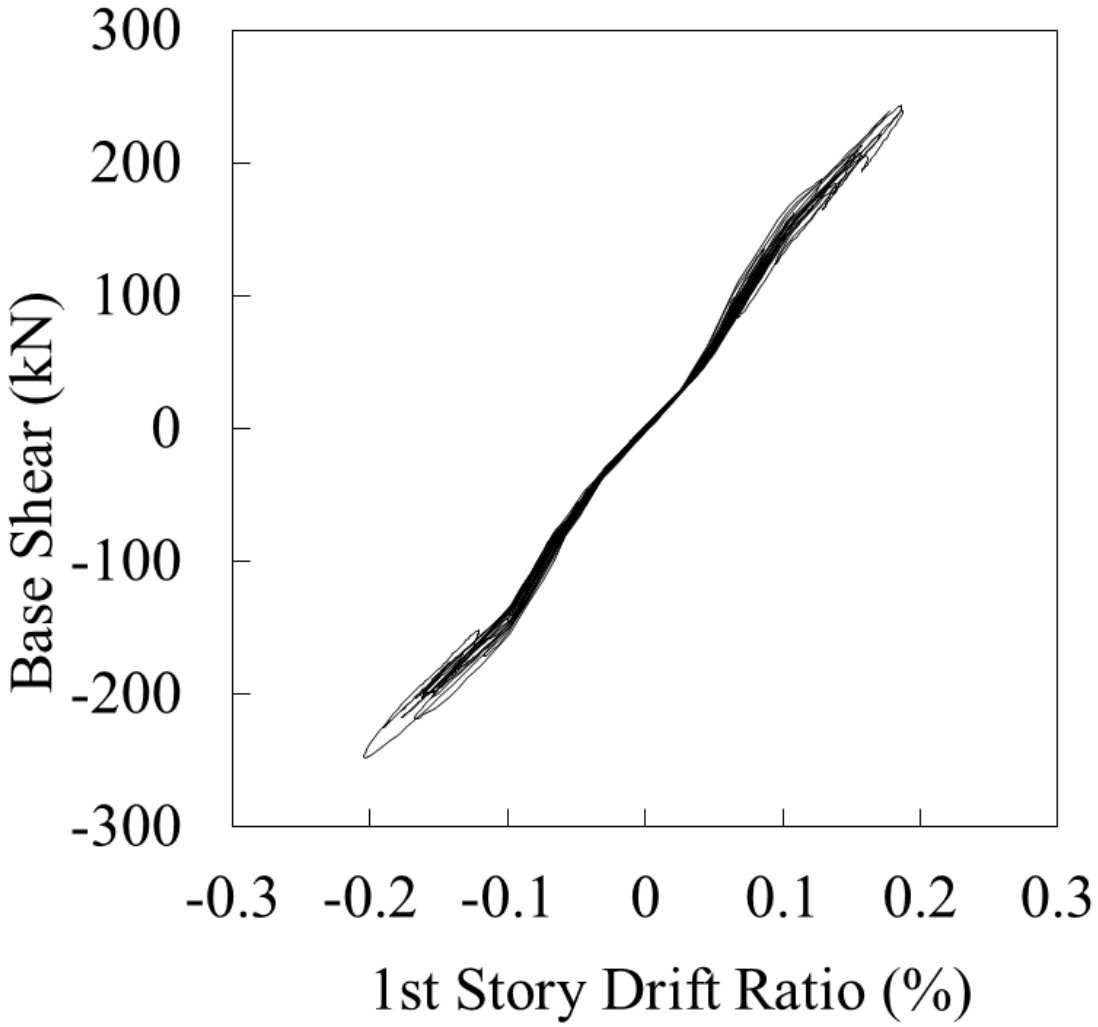

Fig. 10 First story response under a frequent earthquake (Tangshan ground motion)

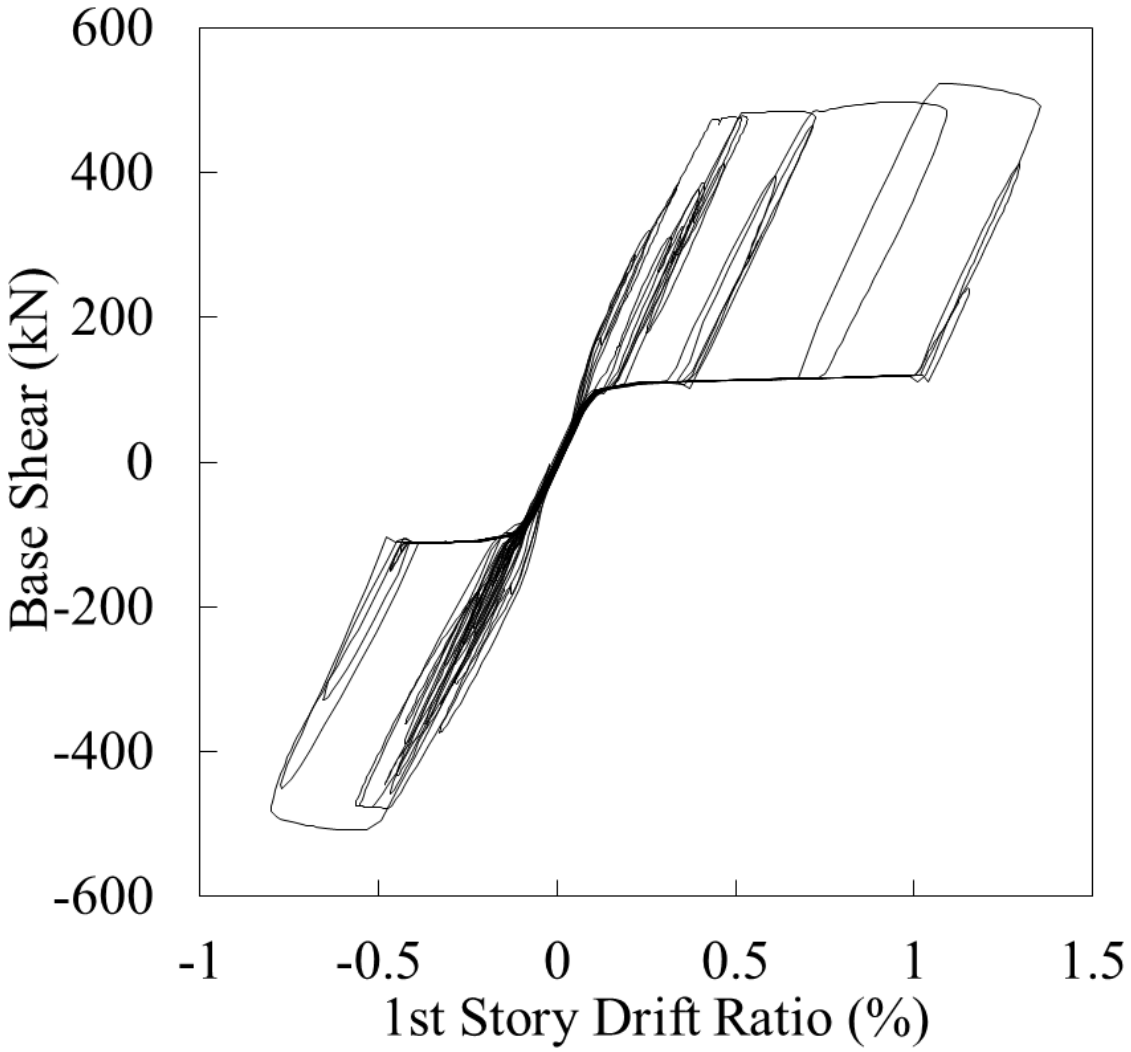

Fig. 11 First story response under a rare earthquake (Tangshan ground motion)

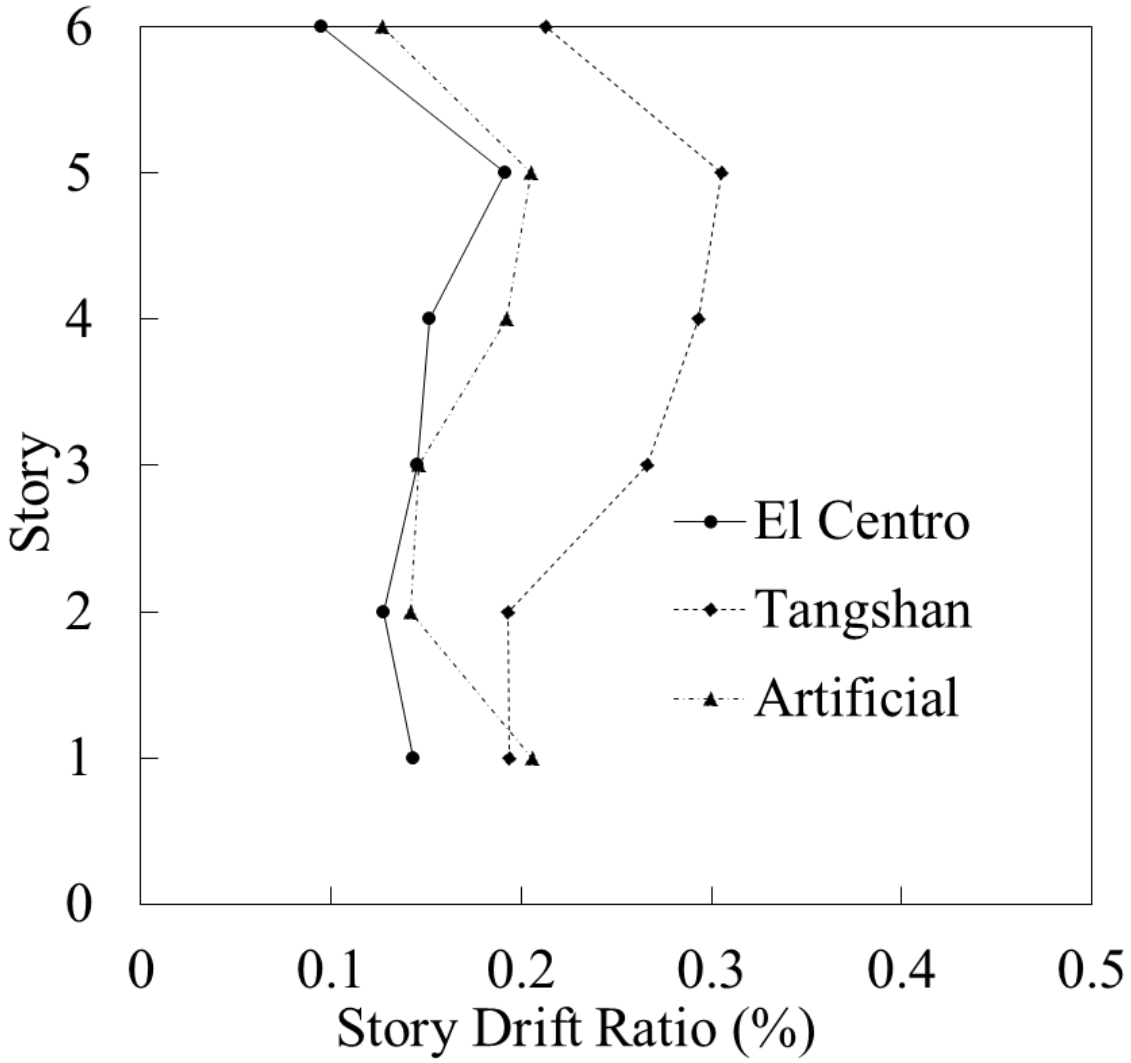

Fig. 12 Maximum story drifts under frequent earthquakes

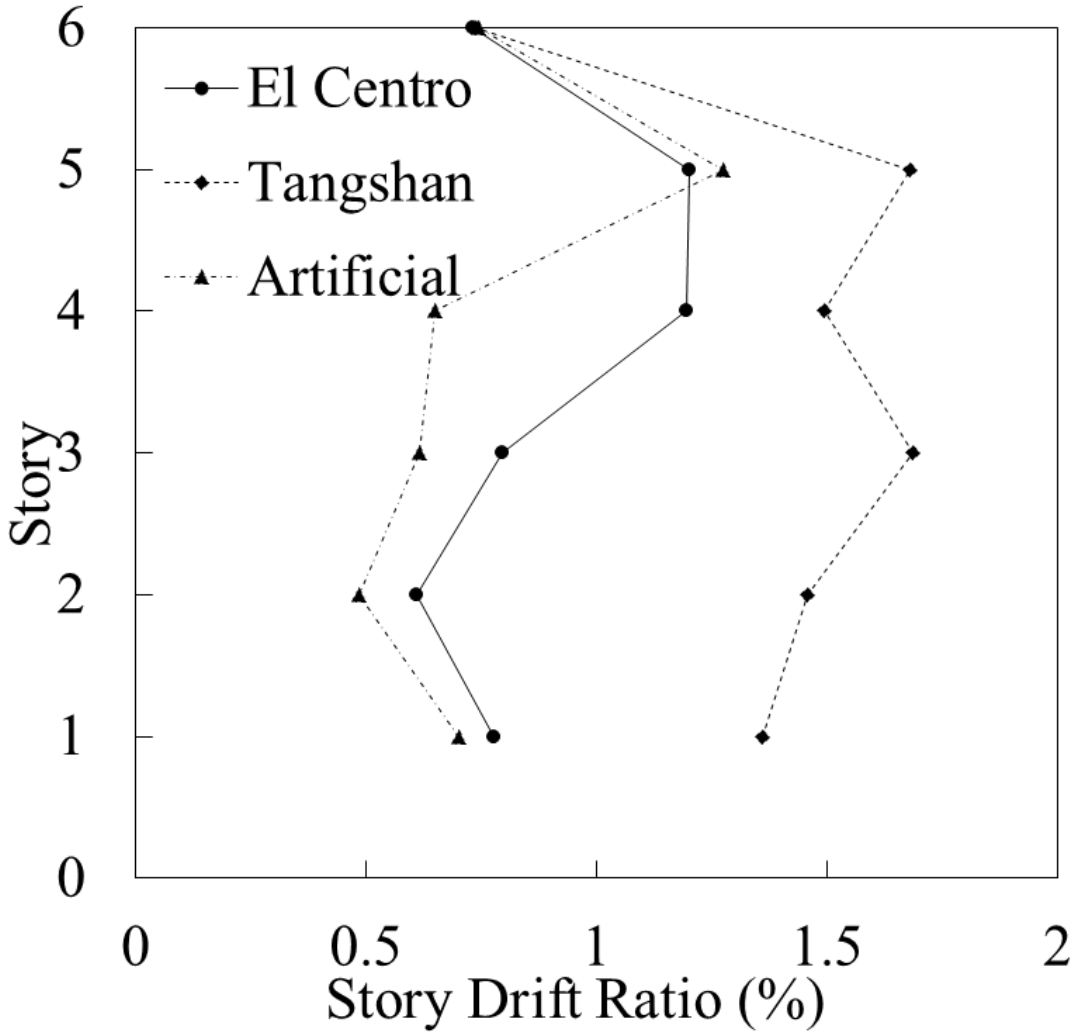

Fig. 13 Maximum story drifts under rare earthquakes

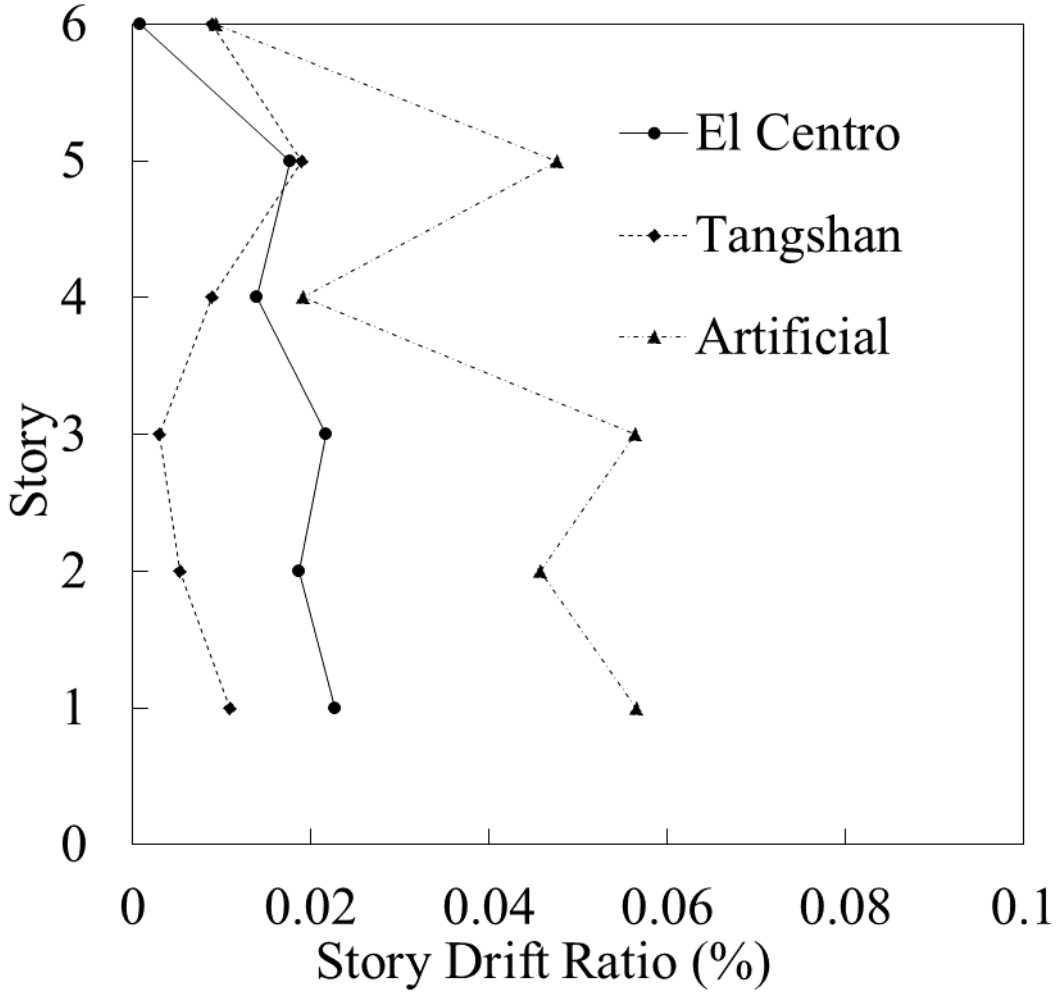

Fig. 14 Residual story drifts after rare earthquakes

Table 1 Design parameters and properties of SCMPs

Properties	Versions of SCMPs			
	SCMP-PT2	SCMP-PT4	SCMP-PT6	SCMP-PT8
N_{PT}	2	4	6	8
A_{PT} (mm^2)	280	560	840	1120
T_0/T_u (%)	32	32	32	32
Panel beam size (mm)	H300×150×10×15	H300×150×10×15	H300×150×20×30	H300×150×20×30
Panel column size (mm)	H250×150×4×6	H300×150×6×8	H300×150×10×14	H300×150×14×18
$k_{i,PTF}$ (N/mm)	6302	10525	17599	20436
k_r (N/mm)	436.8	840	1260	1680
V_{dec} (kN)	37.0	74.1	111.1	148.1
α	0.97	0.95	0.96	0.94
β	0.94	0.93	0.93	0.92
M_e (kNm)	58.8	98.1	160.9	202.1
M_p (kNm)	64.9	110.8	184.6	236.3
M_1 (kNm)	48.9	94.7	142.9	189.2
M_2 (kNm)	70.8	135.9	205.3	271.3

Table 2 Design results of through beams and columns

Components	Cross-sectional dimension (mm)	Axial compression ratio
Through beam	H300×150×4.5×6	—
1st story column	□150×10	0.28
2nd story column	□150×10	0.23
3rd story column	□150×10	0.18
4th story column	□120×8	0.21
5th story column	□120×8	0.14
6th story column	□100×6	0.10

Table 3 Selection results and layout of SCMPs

Stories	P/h (N/mm)	$\Sigma\beta k_r$ (N/mm)	Versions of SCMPs	SCMPs location
1	981.5	1171.8	SCMP-PT6	Middle bay
2	812.1	1171.8	SCMP-PT6	Middle bay
3	642.8	781.2	SCMP-PT4	Middle bay
4	474.3	781.2	SCMP-PT4	Middle bay
5	306.8	410.6	SCMP-PT2	Middle bay
6	139.5	410.6	SCMP-PT2	Middle bay

Table 4 Design results of bracings

Stories	Story shear (kN)	V_{dec} (kN)	V_e (kN)	A_b/mm^2
1	422.0	111.1	359.6	780×2
2	401.9	111.1	304.3	660×2
3	361.8	74.1	304.3	660×2
4	302.0	74.1	276.6	600×2
5	222.6	37.0	276.6	600×2
6	123.6	37.0	249.0	540×2